APPLIED AND ENVIRONMENTAL MICROBIOLOGY, Apr. 1997, p. 1367–1374 Vol. 63, No. 4
0099-2240/97/$04.00+0

Population Structure and Physiological Changes within a Hot Spring Microbial Mat Community following Disturbance

M. J. FERRIS,[1] S. C. NOLD,[1] N. P. REVSBECH,[2] AND D. M. WARD[1]*

Department of Microbiology, Montana State University, Bozeman, Montana 59717,[1] *and Institute of Biological Sciences, University of Aarhus, Aarhus, Denmark*[2]

Received 9 December 1996/Accepted 23 January 1997

The influence of disturbance on a hot spring cyanobacterial mat community was investigated by physically removing the top 3.0 mm, which included the entire cyanobacterial layer. Changes in 16S rRNA-defined populations were monitored by denaturing gradient gel electrophoresis analysis of PCR-amplified 16S rRNA gene segments. Some previously absent cyanobacterial populations colonized the disturbed areas, while some populations which were present before the disturbance remained absent for up to 40 days. Changes in physiological activity were measured by oxygen microelectrode analyses and by $^{14}CO_2$ incorporation into cyanobacterial molecular components. These investigations indicated substantial differences between the disturbed and undisturbed mats, including an unexplained light-induced oxygen consumption in the freshly exposed mat, increased carbon partitioning by phototrophs into growth-related macromolecules, bimodal vertical photosynthesis profiles, and delayed recovery of respiration relative to photosynthesis.

We have used the Octopus Spring cyanobacterial mat as a simple, stable model system in which to investigate principles of microbial community ecology (30, 32). Our molecular and dilution culture studies revealed novel 16S rRNA types that have not been observed in isolates obtained by standard enrichment culture and microscopic analyses (10, 19, 20, 28, 34). 16S rRNA-defined populations exhibit unique spatial distributions and thus represent unique populations of organisms which are probably specialized to different environmental variables (11). Some of these novel populations have been detected repeatedly, while others have only rarely been observed. For instance, we frequently detect A- and B-type cyanobacterial populations directly in the mat and in enrichment cultures established with highly diluted mat inocula (9, 10, 30), whereas other cyanobacterial populations, such as C9 and sequence types I, J, and P, are infrequently detected (31). Even an extensive seasonal survey of population distributions along thermal gradients failed to reveal a pattern of occurrence for these rare populations (11).

It is a common observation in plant and animal ecology that physical perturbations can influence species distributions (2). This occurs when an area occupied by persistent species is cleared, permitting colonization by and growth and succession of new species. In Yellowstone National Park, intense hailstorms or trampling by bison and elk are noted sources of natural stochastic disturbances to shallow microbial mat communities, and anthropogenic disturbances have become an increasing concern (5). We hypothesized that some of the rarely detected bacterial populations may play the role of colonists. As such, one might expect to find them in abundance only in recently disturbed areas, possibly explaining their apparent patchy spatio-temporal distributions (10).

Previous studies addressing the disturbance and reestablishment of this or similar mats have been performed (5, 7). However, these studies did not have the benefit of molecular methods for the detection of bacterial populations. We now realize that this is imperative because many Octopus Spring populations cannot be discerned by traditional techniques, such as microscopy and cultivation (10, 33–36). In the present study, denaturing gradient gel electrophoresis (DGGE) analysis of PCR-amplified 16S rRNA gene segments was used to monitor changes in 16S rRNA-defined bacterial populations following removal of the photosynthetic layer of the mat. DGGE is a technique that can be used to separate equivalently sized double-stranded DNA segments in an acrylamide gel based on sequence differences (1, 17, 18). The resulting banding patterns or "profiles" facilitate the detection of gross changes in population structure and offer the ability to systematically identify individual populations at the 16S rRNA sequence level (9, 17). Microsensor analysis of oxygen microprofiles and distribution of oxygenic photosynthetic and respiratory activities were conducted to correlate changes in microbial populations during recolonization with changes in microbial activity. Physiological differences between cyanobacterial cells within control and disturbed areas were evaluated by measuring the incorporation and partitioning of $^{14}CO_2$ into carbohydrate, protein, lipid, and low-molecular-weight cellular components. Postdisturbance patterns of molecular synthesis were of particular interest, since recent studies have shown that cyanobacterial populations in undisturbed mat communities synthesize primarily storage polymers (e.g., polyglucose) (19) whereas increased synthesis of growth-related molecules would be expected in mat communities recovering from a disturbance event. The overall goal of this study was to enhance our ability to resolve successional events and increase our understanding of the effects of disturbance on microbial mat communities.

MATERIALS AND METHODS

Study sites. The study site was a microbial mat community located in the southernmost effluent channel of Octopus Spring, a thermal pool in the Lower Geyser Basin of Yellowstone National Park, Wyo. (7). The upper surface of the mat contains primarily two cell types, *Synechococcus*-shaped cyanobacterial cells and filamentous bacteria believed to be *Chloroflexus*-like organisms (7, 32). It has recently been demonstrated that phylogenetically diverse Octopus Spring cyanobacterial populations are contained within the *Synechococcus* phenotype (10).

Two sites in the mat were examined. Each was located several meters downstream from the source pool. Here the stream was approximately 25 cm wide and 2.5 cm deep with continuous flow over the experimental sites. The temperature at site 1 varied between 55 and 62°C over a 2-min interval, whereas the temper-

* Corresponding author. Mailing address: Department of Microbiology, Montana State University, Bozeman, MT 59717. Phone: (406) 994-3401. Fax: (406) 994-4926. E-mail: umbdw@gemini.oscs.montana.edu.

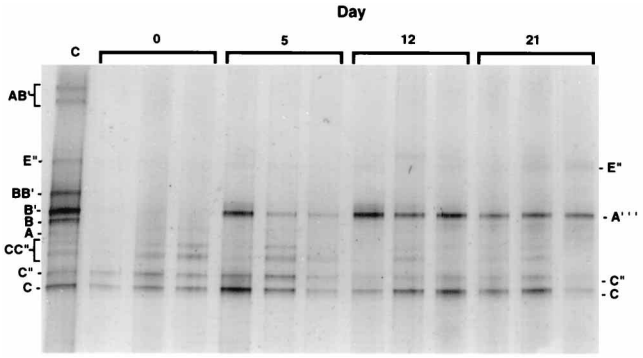

FIG. 1. DGGE profile of a representative undisturbed site 1 mat sample (lane C), and triplicate profiles of site 1 mat immediately (lanes 0) and 5, 12, and 21 days after disturbance. Single letters indicate 16S rRNA sequence types; double letters indicate heteroduplex bands (see the text).

ature at site 2, upstream from site 1, varied between 58 and 62°C over the same interval. At each site, the uppermost 2 to 3 mm of mat was scraped away from areas of approximately 7 by 15 cm (the longer measurement was parallel to the direction of flow) with a spatula. This process visibly removed the green cyanobacterial layer. These scraped areas served as disturbed sites. Adjacent areas a few centimeters upstream from each disturbed site served as undisturbed controls. Microelectrode analyses were conducted toward the downstream side of the disturbed areas to avoid disrupting the boundary between the control and scraped sites.

Sample collection. A no. 4 (7.0-mm-diameter) cork borer was inserted into the mat, and a small cylindrical core was removed. The top of each core (approximately 1.5 mm) was sliced off with a razor blade and placed into a 1.5 ml screw-cap microcentrifuge tube. The samples were stored on dry ice during field collections. During each sampling visit, triplicate cores were collected from both the control and disturbed sites. Within each study site, all samples for DGGE analyses originated within an area of approximately 7.0 by 9.0 cm. Previous DGGE studies indicated that populations are distributed homogeneously within areas of this size with the same temperature range (9). All the samples were collected during a period from June through August 1995 at solar noon ± 2 h. Sampling at site 1 began on 9 June (day 0) and continued on days 5, 12, and 21. Sampling at site 2 began on 18 July (day 0) and continued on days 7, 13, 27, and 40.

***Synechococcus* cell counts.** Counts of *Synechococcus*-shaped cells were performed for samples collected at site 1 on days 0, 5, 12, and 21, using a hemacytometer.

Nucleic acid extraction, PCR, DGGE, and sequencing. The methods used for nucleic acid extraction, PCR amplification conditions, primer sequences, and DGGE have been reported elsewhere (9, 11). The primers have been shown to recover 16S rRNA sequences (*Escherichia coli* positions 1055 to 1406) from six different kingdoms in the domain *Bacteria* (9, 28). Sequence information was obtained from the major (i.e., the most intensely stained) bands that appeared in the DGGE profiles of the control and test sites at the start of the experiment. Thereafter, differential migration of bands produced by possibly different populations was used to identify bands of interest for further sequencing. Since identical band position alone is not an absolute indication of sequence identity, some bands in samples from later time points were also sequenced. DGGE band reamplification, sequencing, and sequence analysis methods have been described previously (9, 11, 16).

Oxygen profiles and photosynthesis. Oxygen profiles in the mat were measured with a Clark-type oxygen microsensor described by Revsbech (25). The sensors used were made so that the difference in signal between stagnant and vigorously stirred air-saturated water was less than 1.5% and the 90% response time to changes in oxygen concentration was less than 0.3 s. The tips were about 6 μm in diameter, and the shaft was made very slim (around 50 μm at a distance of 2 mm from the tip) to minimize physical disturbance by repeated insertion into the same spot. Construction of sensors with both these characteristics results in very low current outputs. Even at 60°C in the spring water, the signals were only about 40 pA for the ambient oxygen concentration (140 μM) and about 2 pA for anoxia. A linear two-point calibration was performed by placing the microsensor tip in the overlying water and dark-incubated anoxic mat. The cyclic temperature changes in the spring resulted in some inaccuracy since both the oxygen concentration in the overlying water and the sensitivity of the sensor were affected by these changes. Thus, the current from the sensor could be read with excellent accuracy but the absolute values are accurate only within a range of ±10%. The microsensor was inserted vertically from above with a manually operated micromanipulator, and the signal was recorded on a strip-chart recorder. All measurements were conducted only in bright sunlight at solar noon ± 2 h, and all oxygen profiles were measured after the mat had been exposed to constant illumination for a minimum of 15 min. The light intensity during sampling was ca. 65,000 lux (LX-101 lux meter; Lutron).

Photosynthetic activity was measured by the light-dark shift technique (26). The microsensor was positioned in the photosynthetic layer, and the change in oxygen concentration during a short period of darkening was recorded. It has been shown that the spatial resolution of this method is about 0.1 mm when the change in signal is recorded within 1 s after the light is extinguished (13). Circumstances in the field necessitated a dark period of about 2 s to accurately record the change, and since the diffusion coefficient for oxygen at 60°C is 2.1 times higher than at room temperature, the spatial resolution of our measurements was about 0.2 mm. The parameter obtained by this procedure is gross photosynthesis; therefore, to obtain net photosynthetic rates, we would have to subtract the simultaneously occurring respiratory activity in the same layer.

Darkening of the mat was accomplished with a 12- by 12-cm black plastic box with the bottom removed. The upper surface of the box was 3 cm high at the end facing the Sun (south) and 5 cm high at its north side. Thus, the upper surface was almost perpendicular to the incoming sunlight. Sunlight entered the box through a 6- by 6-cm square opening in the upper surface. A 1- by 1-cm extension of the 6- by 6-cm opening was located at the center of the 6-cm side facing north. This provided a small opening through which the oxygen microsensor probe was inserted during experiments that required the 6- by 6-cm opening to be covered. The box was held about 0.5 cm above the mat surface by steel rods fixed to the outside of the box. Various light intensities were achieved inside the box by placing one to three layers of translucent tracing paper over the 6- by 6-cm opening. Darkening was accomplished by covering the opening with a sheet of black plastic. It was necessary to move the box about every hour to keep the microsensor insertion point within the center of the area illuminated through the 6- by 6-cm opening.

Radiolabeling and cell fractionation. Triplicate samples from both the scraped and control areas at site 1 were collected with a no. 4 cork borer as described above on days 0, 5, 13, and 21 and transferred to 4.0-ml glass vials containing 3.0 ml of water from the collection site. The samples were then incubated for 3 h at ambient water temperature and light intensities in the presence of 1.0 μCi of ^{14}C-labeled sodium bicarbonate (54.6 mCi/mmol; New England Nuclear). Following incubation, the samples were frozen on dry ice to stop biological activity. Cells were separated from unincorporated radiolabel by centrifugation (20 min at 15,000 × *g*) and washed once with sterile water to remove unincorporated $^{14}CO_2$; 98.5% ± 1.7% (mean ± standard deviation [SD], n = 21) removal of unincorporated ^{14}C was measured in the first cell wash. The major end products of photosynthesis were determined by partitioning cellular carbon into chloroform-soluble (lipid), methanol-water-soluble (low-molecular-weight metabolites), hot trichloroacetic acid-soluble (carbohydrate), and hot trichloroacetic acid-insoluble (protein) fractions by the method of Li et al. (15) as modified by Fitzsimons et al. (12). The radioactivity in each of these fractions was determined by liquid scintillation counting as previously described (21). Total incorporated ^{14}C was calculated by adding the radioactivity detected in each fraction. By comparison with whole-cell incorporation, recovery of ^{14}C by this method was determined to be 94.6% ± 13.2% (mean ± SD, n = 7). The extent of radiolabel incorporation into cellular material in disturbed and undisturbed regions of the mat was compared by a two sample t test.

Nucleotide sequence accession number. The new sequence reported here (type A‴) has been submitted to GenBank and assigned accession number U88530.

RESULTS

Microscopic cell counts. At site 1, counts of *Synechococcus*-shaped cells in the undisturbed mat were around 6.2 × 10^9 cells/ml. On day 0, just after scraping away the surface layer,

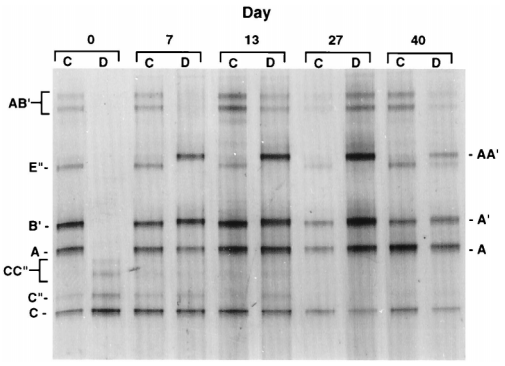

FIG. 2. DGGE profiles of representative control (lanes C) and disturbed (lanes D) site 2 samples immediately (day 0) and 7, 13, 27, and 40 days after disturbance. Single letters indicate 16S rRNA sequence types; double letters indicate heteroduplex bands (see the text).

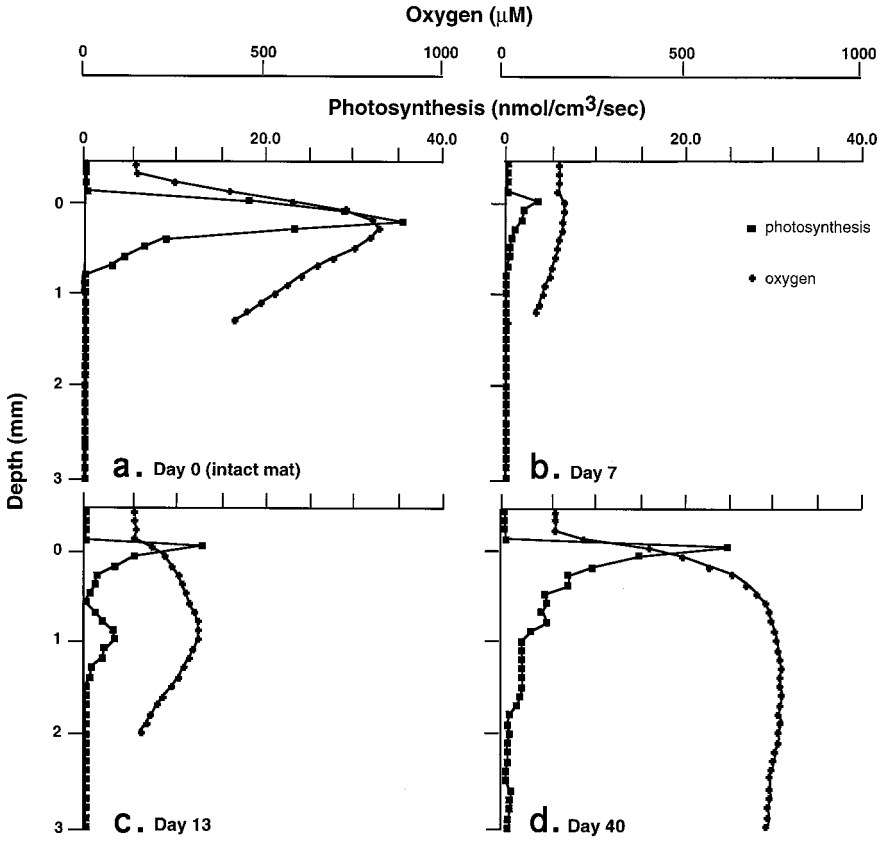

FIG. 3. Vertical profiles of oxygen and gross oxygenic photosynthesis before (day 0) (a) and 7 (b), 13 (c), and 40 (d) days after disturbance of the site 2 mat.

microscopic fields were dominated by filamentous cell forms to the extent that meaningful counts of the few *Synechococcus*-shaped cells that may have been present could not be made. On days 5, 12, and 21, the counts were 1.6×10^8, 3.2×10^8, and 5.5×10^8 cells/ml, respectively.

DGGE profiles. Major bands in DGGE profiles of replicate samples were essentially identical. An example of this can be seen in Fig. 1, where banding patterns of replicate samples were the same on a given sampling day. DGGE profiles of samples from control sites were also constant over time, except that band C″ from the site 2 sample seemed to diminish with time and there was some variability in the formation of the AB′ heteroduplex bands (artifacts containing one strand from each of two closely related sequences [11]) (Fig. 2). In contrast, the DGGE profiles of disturbed areas appeared notably different than those of the controls.

With one exception (noted below), the sequences of all DGGE bands in this study have been previously detected in the Octopus Spring mat (9, 11, 32). The identity of each band is thus indicated by a letter that corresponds to an Octopus Spring 16S rRNA sequence type. Bands A, A′, B, and B′ are contributed by cyanobacterial populations; bands C and C″ are contributed by green nonsulfur bacterium-like populations, and band E″ is contributed by a green sulfur bacterium-like population (Fig. 1 and 2). Heteroduplex bands are labeled with two letters that correspond to their component sequences (11). The sequences of three individual bands (labeled A‴ in Fig. 1 [site 1]), exhibited one nucleotide difference from that of band A′ (Fig. 2 [site 2]).

Site 1 originally contained major bands identified as Octopus Spring cyanobacterial types B and B′, green nonsulfur bacterium-like sequences C and C″, and green sulfur bacterium-like sequence E″. A heteroduplex band, BB′, was present above the B′ band. Faint bands that correspond to cyanobacterial type A and to the AB′ heteroduplexes were also seen (Fig. 1, lane C). This pattern was typical of samples in this temperature range (11). Immediately following the removal of the surface layer, the cyanobacterial bands were absent from the DGGE profile, as was band E″. Bands C and C″ were present on day 0 and throughout the experiment. Two bands labeled CC″ were also observed on day 0 just after removal of the surface layer. Our best reamplification evidence suggests that these are heteroduplex molecules composed of C and C″, but this could not be established with certainty (11). On day 5, an A′-like cyanobacterial band (A‴), which was not detected before the disturbance, appeared in the profile; it remained present through day 21. The other cyanobacterial bands, most notably the originally prominent B and B′ bands, remained absent. A faint E″ band was evident by day 21.

Site 2 initially contained cyanobacterial bands A and B′, green nonsulfur bacterium-like bands C and C″, and the green sulfur bacterium-like sequence, band E″. This pattern was typical given the slightly higher temperature range and upstream location relative to site 1 (11). In addition, two AB′ heteroduplex bands were present as the uppermost bands in the gel (Fig. 2). As at site 1, the cyanobacterial bands were absent from profiles immediately after removal of the surface layer. A cyanobacterial band A′, which was not detected before the disturbance, appeared on day 7 along with band A and the heteroduplex band AA′. Heteroduplex bands AB′ were faintly visible in the disturbed site on days 13 and 40 and are clearly visible in the disturbed site on day 27, indicating the presence

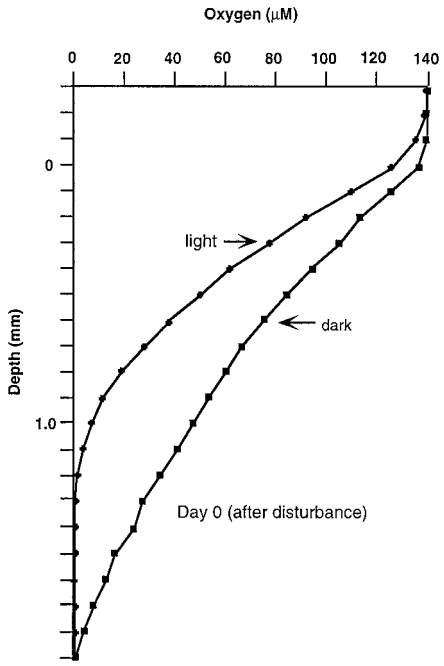

FIG. 4. Vertical profiles of oxygen penetration into the site 2 mat measured immediately after disturbance in full sunlight and darkness.

of the B′ population. Band E″ was absent on day 0, but a faint band corresponding in position and sequence to band E″ reappeared in the scraped site on day 40. Band C was present throughout the experiment. Band C″ appeared to diminish with time.

Oxygen and photosynthesis. The oxygen and photosynthetic activity profiles of site 2 at midday under full sunlight are shown in Fig. 3. Similar results were observed at site 1 (data not shown). Prior to removal of the photosynthetic layer, an intense photosynthetic activity of up to 35 nmol cm^{-3} s^{-1} at 0.2-mm depth in the undisturbed mat resulted in a peak oxygen concentration of 820 μM at 0.3 mm deep (Fig. 3a). Oxygen consumption in the deeper layers resulted in a decrease to 50% of the peak concentration only 1 mm below the maximum. The photosynthetic zone was about 0.9 mm thick, and the integrated photosynthetic activity was 1.29 nmol cm^{-2} s^{-1}. Immediately after removal of the photosynthetic layer, photosynthetic activity could not be detected by use of the microsensors; in fact, an apparent light-induced consumption of oxygen was observed, as noted in a comparison of light and dark profiles (Fig. 4). After 7 days, a pale green layer had developed at the surface of the mat and a peak photosynthetic rate of 3.3 nmol cm^{-3} s^{-1} was detected in the top layer (Fig. 3b). Low activities could be detected down to a depth of 0.7 mm, but the total activity (0.086 nmol cm^{-2} s^{-1}) was barely able to raise the oxygen concentration above that found in the overlying water (154 μM found at 0.2-mm depth). After 13 days (Fig. 3c), the photosynthetic activity had increased considerably to 0.40 nmol cm^{-2} s^{-1} with a peak activity of 12.8 nmol cm^{-3} s^{-1} in the surface layer. The photosynthetic activity had a bimodal appearance with a second peak at 1-mm depth and activity could be detected down to 1.5-mm depth. The maximum oxygen concentration was associated with the deepest maximum in photosynthetic activity, where a concentration of 310 μM was detected. After 40 days, the depth-integrated photosynthetic activity was 1.04 nmol cm^{-2} s^{-1} and was thus back to the normal range (Fig. 3d). The distribution of the activity was, however, quite different from that in the control, since activity could be detected down to a depth of 3 mm. The activities at depth were low but apparently were sufficient to balance respiration, as evidenced by the virtually linear (and vertical) oxygen profile from 1 to 3 mm deep. The integrated photosynthetic rates as a function of incubation time after removal of the top layer are shown in Fig. 5.

Respiratory rates and oxygen profiles in the dark. From the data on oxygen and photosynthesis 7 days after scraping (Fig. 3b), it can be seen that photosynthetic activity almost balanced respiration within the mat, resulting in an almost vertical oxygen profile across the water-mat interface. If photosynthesis exactly balanced respiration, the profile would be vertical. Since there was a slight excess of oxygen, photosynthesis under these conditions must have slightly exceeded respiration, so that the integrated rate of photosynthesis (0.086 nmol cm^{-2} s^{-1}) would slightly overestimate the rate of respiration. When we reduced photosynthesis by shading the mat with one layer of tracing paper, an oxygen deficit resulted (i.e., decreasing oxygen concentration with depth rather than a vertical profile), indicating that respiration then exceeded photosynthesis, and the photosynthetic rate under these conditions (0.031 nmol cm^{-2} s^{-1}) underestimated the rate of respiration. The true rate of respiration was judged to be between these extremes (i.e., 0.05 nmol cm^{-2} s^{-1}). We used this general approach to estimate the respiratory rates for all postdisturbance time points (Fig. 5).

The most inaccurately determined rates are those after 40 days, since even shading with three layers of paper did not cause near-vertical oxygen profiles across the mat-water interface, but all estimates are probably correct to within ±20%. It is evident that removal of the photosynthetic layer reduced the respiratory activity considerably, and the activity had not fully recovered after 40 days (Fig. 5), although without replication this is not a quantitative observation. The effect of disturbance on respiratory activity was, however, also evident from the oxygen profiles in scraped mat during dark incubation, where both the oxygen gradient in the surface layer (the steeper the gradient, the higher the respiratory activity) and oxygen penetration (the shallower the oxygen penetration, the higher the

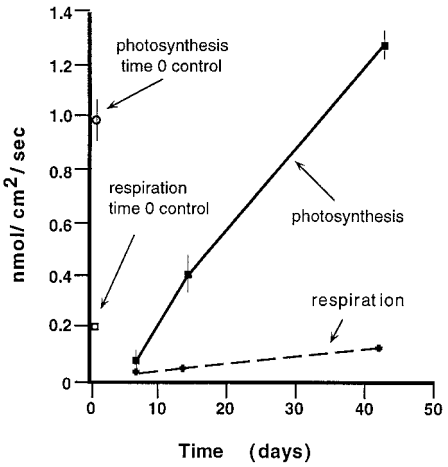

FIG. 5. Depth-integrated photosynthetic rates and estimated respiration rates in the undisturbed site 2 mat on day 0 and as a function of time after removal of the top layer. Bars indicate the standard error (n = 6). Respiration rates were not replicated.

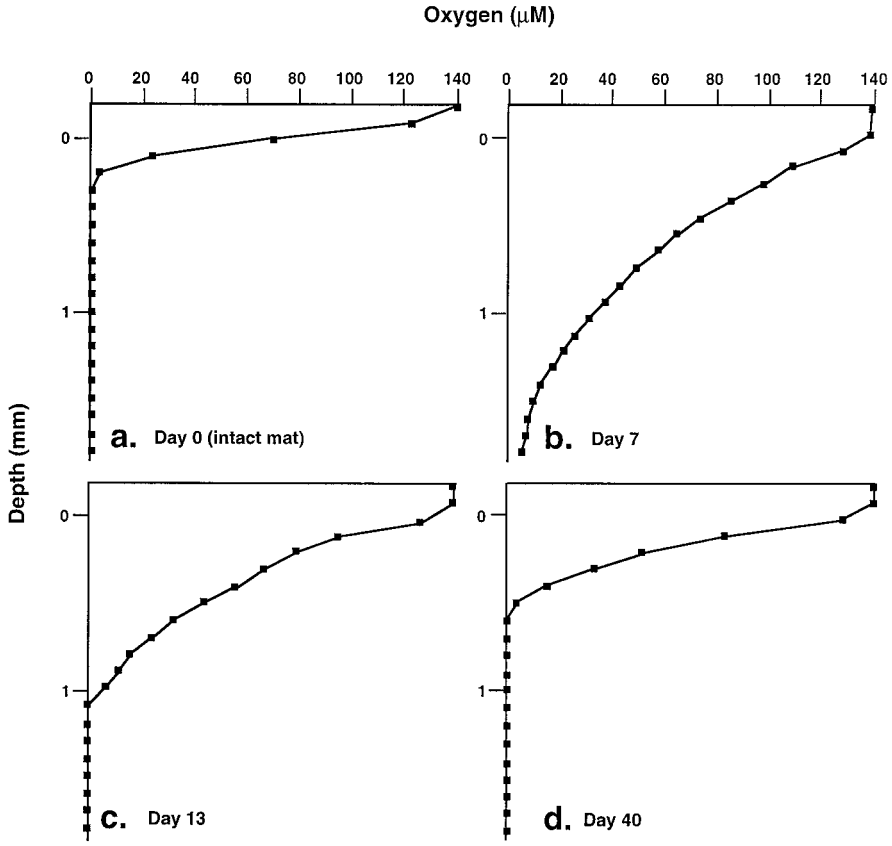

FIG. 6. Vertical oxygen profiles measured under dark conditions in the site 2 mat before (day 0) (a) and 7 (b), 13 (c), and 40 (d) days after the disturbance.

respiratory activity) indicate reduced respiratory activity throughout the 40-day period (Fig. 4 and 6).

Partitioning of $^{14}CO_2$ into cell components. Samples from the site 1 control area incorporated between 3.9×10^5 and 5.97×10^5 dpm of $^{14}CO_2$ core^{-1} (Fig. 7A, top panel) and partitioned the majority of photosynthetically fixed carbon into the polysaccharide fraction (67 to 79% of the total incorporated radiolabel) during the experimental period (Fig. 7A, bottom panel). In contrast, cells in the scraped region of the mat incorporated significantly less carbon than did those in the controls on all sampling dates ($P < 0.0305$, $n = 3$) and displayed an increase in carbon incorporation between days 5 and 21 (Fig. 7B, top panel). In addition, cells in the disturbed region of the mat displayed variable patterns of carbon partitioning between molecular components (Fig. 7B, bottom panel). On day 5, $^{14}CO_2$ was partitioned nearly equally into protein, low-molecular-weight compounds, and carbohydrate. Carbon incorporation into the carbohydrate fraction increased from days 5 to 21, and carbon incorporation into the protein and low-molecular-weight fractions decreased over the same interval. By day 21, the majority of the radiolabel associated with cellular material was detected in the polysaccharide fraction.

DISCUSSION

DGGE banding patterns, oxygen and photosynthesis profiles, and carbon fixation measurements indicated that substantial changes in the Octopus Spring mat community occurred following removal of the surface layers. The freshly exposed undermat appeared red-orange. Microscopic examination of this layer immediately after scraping revealed almost exclusively filamentous cell forms with few *Synechococcus*-shaped cells, indicating that most of the cyanobacteria had been eliminated. This is consistent with the absence of cyanobacterial bands in the DGGE profiles and the absence of detectable oxygen production. In addition, a light-dependent consumption of oxygen was observed in the freshly exposed undermat. This phenomenon has been reported to occur in deeper layers of the Solar Lake microbial mat (i.e., >30 mm below the surface freshly exposed by removal of the overlying mat layers) (14). In our experiment, the newly exposed undermat was about 3 mm beneath the original mat surface. No mechanism for this phenomenon has been elucidated.

Recovery of *Synechococcus* mats following disturbances has been noted previously. In some cases, recovery was measured following an artificial disturbance, such as the application of an opaque layer of silicon carbide to the surface of the mat (3, 7) and a prolonged period of darkening which resulted in complete washout of the *Synechococcus*-shaped cells (3). In one case, recovery was measured after an intense hailstorm had completely scoured away the mat, leaving behind an area of cleared substratum (5). Our observation of an olive-green film composed of *Synechococcus*- and *Chloroflexus*-shaped cells covering the disturbed sites within a few days after the disturbance was consistent with observations made in the above studies. Our cell counts were essentially the same as those made by Brock and Brock following hailstorm damage to the microbial mat in neighboring Mushroom Spring (5).

We were able to take advantage of DGGE, microsensors, and radiolabel partitioning methods to provide a more detailed

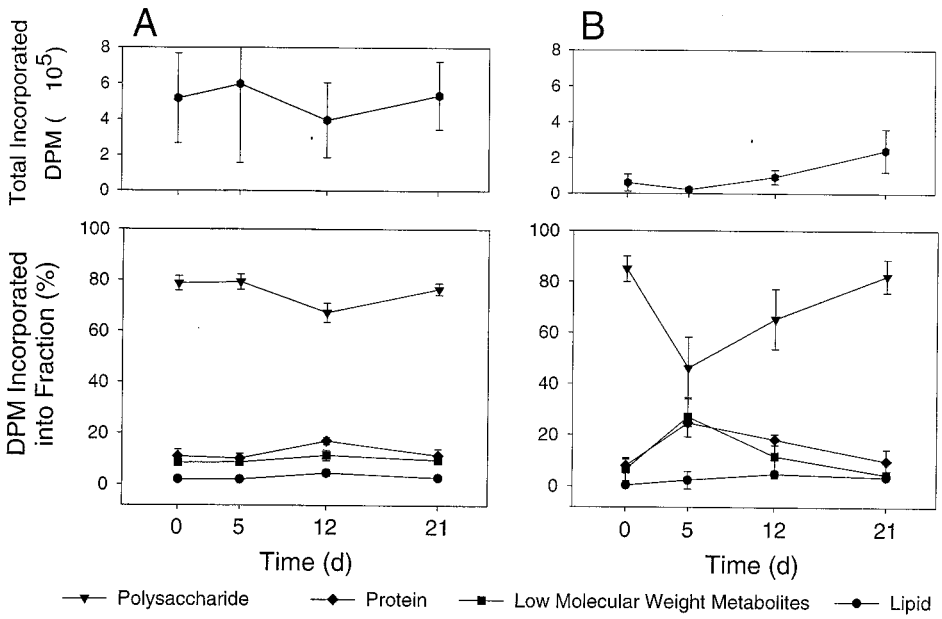

FIG. 7. Patterns of $^{14}CO_2$ incorporation (top panels) and partitioning into carbohydrate (triangles), protein (diamonds), lipid (circles), and low-molecular-weight metabolite (squares) cellular fractions (bottom panels). (A) Control area; (B) site 1 immediately (day 0) and 5, 12, and 21 days after disturbance. Error bars represent 95% confidence intervals about the mean ($n = 3$).

view of the recovery of the cyanobacterial community and its activity. Low levels of oxygen production and photosynthesis at both sites 1 and 2 on days 5 and 7, respectively (Fig. 3b [site 2]), were consistent with the re-formation of a cyanobacterial layer shortly after the disturbance events. The DGGE profiles indicated that the populations in the newly established layer differed from those in the undisturbed sites. Some populations present before the disturbance were absent in the new layer, and some populations that were not detected before the disturbance appeared over time. New cyanobacterial populations, A′ and A‴, initially colonized the freshly exposed undermat at both of the disturbed sites. This occurred in the absence of both originally prominent cyanobacterial populations, B and B′, at site 1 and in combination with one of the originally prominent cyanobacterial populations, A, at site 2. The reappearance of the AB′ heteroduplex bands at later time points at site 2 indicated that the B′ cyanobacterial population had also begun to recolonize this area. The A′ and B′ bands are difficult to resolve when they both appear in the same lane, but the differential migration of their heteroduplex forms aided in their detection.

Two green nonsulfur bacterium-like populations, C and C″, and a green sulfur bacterium-like population, E″, were initially present at each site. Removal of the surface layer appeared to eliminate the E″ population in both cases, suggesting that it inhabits only the upper cyanobacterial layer of the mat. In contrast, the C and C″ bands appeared in the intact mat and remained detectable in the undermat after scraping, suggesting that these green nonsulfur bacterium-like populations may reside deeper in the vertical interval. These results are consistent with the vertical positions of E-like and C-like populations in a similar mat community (Mushroom Spring) (23). The bimodal photosynthesis profile 13 days following disturbance of site 2 may indicate a vertical structure related to different cyanobacterial populations, also consistent with unpublished observations (23). The E″ band had returned to detectable levels by day 40 at site 2, and a faint E″ band had also appeared at site 1 by day 21, suggesting that over time the E″ population had begun to reestablish itself at both sites.

The observation that A′-like cyanobacterial populations (A′ and A‴) were involved in recolonization of both areas invokes speculation about why this was so, especially since these populations were not initially observed at either site. Establishment of a population in the scraped areas probably involves a combination of immigration and reproduction. Immigration may occur by dispersal of cells from upstream areas or by the active migration of motile cells into the disrupted site (24). It is of note that the A′ cyanobacterial population is routinely detected upstream, near the uppermost temperatures at which the cyanobacterial mat is visible (9, 11). Thus, dispersal from a hotter upstream site to the downstream disturbed sites might account for the appearance of this population. However, if dispersal from upstream was the dominant factor controlling the appearance of populations in the scraped sites, one would anticipate the appearance of the original populations, since they, too, were present immediately upstream in the control areas.

Our initial presumption that thermophilic *Synechococcus* populations are essentially immobile and thus incapable of actively traversing the scraped areas (6) was revised by the recently demonstrated gliding motility of several Octopus Spring *Synechococcus* isolates (24). Recolonization of the disturbed areas by gliding *Synechococcus* cells would also seem to favor cells that are closest to a newly exposed site, i.e., the original populations. While it is not possible to determine whether motility played a role in this study, the absence of the B and B′ populations during recolonization of site 1 suggests that motility was not a key factor in their case.

It seems more plausible that A′-like cells are, by some means, more capable of establishing themselves in the exposed site. Investigation of the environment in which A′ cells are typically found leads to several possible explanations. The highest-temperature regions of the Octopus Spring mat are visibly thinner than the downstream portions, consisting of a

thin, pale green film coating the channel substratum. It may be that the A′ cells in these thin regions can tolerate higher visible and UV light intensities and thus may be better able to cope with equivalent conditions present in freshly exposed sites. Alternatively, the uppermost temperature extremes may select for populations that are capable of rapidly recolonizing the fringe areas where cells are intermittently eliminated by occasional surges of hot water from the source pool. Thus, A′ may be an efficient colonizer, able to rapidly move into and grow in areas free of competing cells.

Since B and B′ cyanobacterial populations, which differ by only a single nucleotide in 300 positions analyzed, represent different ecotypes (11), we hypothesize that the same may be true for the A′ and A‴ cyanobacterial colonist populations. Given the highly conserved nature of the 16S rRNA sequence, it is even possible that the A′ population detected as a colonist is not identical to the A′ population found in the undisturbed mat at higher temperatures. This can be verified only by analyzing higher-resolution genetic markers.

Although we had hypothesized that some of the more rarely detected 16S rRNA-defined cyanobacterial populations might establish themselves in disturbed sites as colonizer species, this was not observed. Previous DGGE surveys of the effluent channel over a seasonal interval also failed to detect these rare populations (11). It may be that such populations are simply not abundant and are not efficient colonizer species (11). However, the possibility that methodological biases prevent the detection of the 16S rRNA genes of these populations cannot be excluded (8, 22, 27, 29).

It is likely that cell division played a significant role in the reestablishment of *Synechococcus* populations. That growth of *Synechococcus* cells had occurred at the disturbed sites can be inferred from the $^{14}CO_2$-labeling results. Cells in the disturbed site had allocated a higher proportion of fixed carbon into growth-related cellular components by days 5 and 12 than had those in the undisturbed control area, suggesting that *Synechococcus* cells within the scraped sites were initially dividing more frequently than those in the undisturbed mat. By day 21, carbon partitioning in the disturbed site was nearly the same as in the undisturbed control area, suggesting that the rate of cell growth had begun to decrease (21). $^{14}CO_2$ incorporation immediately following scraping was unlikely to have been due to cyanobacterial autotrophy, because cyanobacteria had just been removed and no oxygenic photosynthesis was detected.

By the end of the experiment, 21 days for site 1 and 40 days for site 2, the original population structures had not been reestablished at either of the disturbed sites. Oxygen production and penetration occurred throughout a considerably greater depth interval than in the intact mat. Likewise, incorporation of $^{14}CO_2$ remained below initial levels. Respiratory activity was not yet in balance with oxygenic photosynthesis. The time required for full recovery of the microbial mat community remains to be determined.

Clearly, disturbances resulting from our anthropogenic influence affected the composition, structure, and function of this microbial community. The same effect can be presumed to occur after natural disturbances. The stability in community structure observed over a seasonal cycle (11) suggests that such disturbances may not be frequent, although in the month following the completion of this work, the entire mat was heavily damaged by hail, which may have caused the types of changes we observed. Extensive anthropogenic sampling might result in similar effects.

ACKNOWLEDGMENTS

We thank Bob Lindstrom and the Yellowstone National Park Service for their support.

This work was supported by a grant (BSR-9209677) from the National Science Foundation.

REFERENCES

1. **Abrams, E. S., and V. P. Stanton.** 1992. Use of denaturing gradient gel electrophoresis to study conformational transitions in nucleic acids. Methods Enzymol. **212:**71–104.
2. **Begon, M., J. L. Harper, and C. R. Townsend.** 1990. Ecology: individuals, populations, and communities, 2nd ed. Blackwell Scientific Publications, Boston, Mass.
3. **Brock, T. D.** 1978. Thermophilic microorganisms and life at high temperatures. Springer-Verlag KG, Berlin, Germany.
4. **Brock, T. D., and M. L. Brock.** 1968. Measurement of steady-state growth rates of a thermophilic alga directly in nature. J. Bacteriol. **95:**811–815.
5. **Brock, T. D., and M. L. Brock.** 1969. Recovery of a hot spring community from a catastrophe. J. Phycol. **5:**75–77.
6. **Castenholz, R. W., and J. B. Waterbury.** 1989. Oxygenic photosynthetic bacteria, p. 1710–1806. *In* J. T. Staley, M. P. Bryant, N. Pfennig, and J. G. Holt (ed.), Bergey's manual of systematic bacteriology, vol. 3. The Williams & Wilkins Co., Baltimore, Md.
7. **Doemel, W. N., and T. D. Brock.** 1977. Structure, growth, and decomposition of laminated algal-bacterial mats in alkaline hot springs. Appl. Environ. Microbiol. **34:**433–452.
8. **Farrelly, V., F. A. Rainey, and E. Stackebrandt.** 1995. Effect of genome size and *rrn* gene copy number on PCR amplification of 16S rRNA genes from a mixture of bacterial species. Appl. Environ. Microbiol. **61:**2798–2801.
9. **Ferris, M. J., G. Muyzer, and D. M. Ward.** 1996. Denaturing gradient gel electrophoresis profiles of 16S rRNA-defined populations inhabiting a hot spring microbial mat community. Appl. Environ. Microbiol. **62:**340–346.
10. **Ferris, M. J., A. L. Ruff-Roberts, E. D. Kopczynski, M. M. Bateson, and D. M. Ward.** 1996. Enrichment culture and microscopy conceal diverse thermophilic *Synechococcus* populations in a single hot spring microbial mat habitat. Appl. Environ. Microbiol. **62:**1045–1050.
11. **Ferris, M. J., and D. M. Ward.** 1997. Seasonal distributions of dominant 16S rRNA-defined populations in a hot spring microbial mat examined by denaturing gradient gel electrophoresis. Appl. Environ. Microbiol. **63:**1375–1381.
12. **Fitzsimons, A. G., C. E. Gibson, and P. A. W. Elliot.** 1993. The fractionation of cell components in *Oscillatoria agardhii*: an audit of procedures. Hydrobiologia **268:**163–168.
13. **Glud, R. N., N. B. Ramsing, and N. P. Revsbech.** 1992. Photosynthesis and photosynthesis-coupled respiration in natural biofilms quantified with oxygen microsensors. J. Phycol. **28:**51–60.
14. **Jørgensen, B. B., Y. Cohen, and N. P. Revsbech.** 1988. Photosynthetic potential and light-dependent oxygen consumption in a benthic cyanobacterial mat. Appl. Environ. Microbiol. **54:**176–182.
15. **Li, W. K. W., H. E. Glover, and I. Morris.** 1980. Physiology of carbon photoassimilation by *Oscillatoria thiebautii* in the Caribbean Sea. Limnol. Oceanogr. **25:**447–456.
16. **Maidak, B. L., N. Larsen, M. J. McCaughey, R. Overbeek, G. J. Olsen, K. Fogel, J. Blandy, and C. R. Woese.** 1994. The Ribosomal Database Project. Nucleic Acids Res. **22:**3485–3487.
17. **Muyzer, G., S. Hottentrager, A. Teske, and C. Wawer.** 1996. Denaturing gradient gel electrophoresis of PCR-amplified genes coding for 16S rDNA—a new molecular approach to analyze the genetic diversity of mixed microbial communities, p. 3.4.4.1–3.4.4.22. *In* A. D. L. Akkermans, J. D. van Elsas, and F. J. de Bruijn (ed.), Molecular microbial ecology manual. Kluwer Academic Publishers, Dordrecht, The Netherlands.
18. **Myers, R. M., T. Maniatis, and L. S. Lerman.** 1987. Detection and localization of single base changes by denaturing gradient gel electrophoresis. Methods Enzymol. **155:**501–527.
19. **Nold, S. C., E. D. Kopczynski, and D. M. Ward.** 1996. Cultivation of aerobic chemoorganotrophic proteobacteria and gram-positive bacteria from a hot spring microbial mat. Appl. Environ. Microbiol. **62:**3917–3921.
20. **Nold, S. C., and D. M. Ward.** 1995. Diverse *Thermus* species inhabit a single hot spring microbial mat. Syst. Appl. Microbiol. **18:**274–278.
21. **Nold, S. C., and D. M. Ward.** 1996. Photosynthate partitioning and fermentation in hot spring microbial mat communities. Appl. Environ. Microbiol. **62:**4598–4607.
22. **Rainey, F. A., N. Ward, L. I. Sly, and E. Stackebrandt.** 1994. Dependence of the taxonomic composition of clone libraries for PCR-amplified naturally occurring 16S rDNA on the primer pair and the cloning system used. Experientia **50:**789–801.
23. **Ramsing, N. B., M. J. Ferris, and D. M. Ward.** Unpublished results.
24. **Ramsing, N. B., M. J. Ferris, and D. M. Ward.** Light-induced motility of thermophilic *Synechococcus* isolates from Octopus Spring, Yellowstone National Park. Submitted for publication.

25. **Revsbech, N. P.** 1989. An oxygen microelectrode with guard cathode. Limnol. Oceanogr. **34:**472–476.
26. **Revsbech, N. P., and B. B. Jørgensen.** 1986. Microelectrodes: their use in microbial ecology. Adv. Microb. Ecol. **9:**293–352.
27. **Reysenbach, A. L., L. J. Giver, G. S. Wickham, and N. R. Pace.** 1992. Differential amplification of rRNA genes by polymerase chain reaction. Appl. Environ. Microbiol. **58:**3417–3418.
28. **Santegoeds, C. M., S. C. Nold, and D. M. Ward.** 1996. Denaturing gradient gel electrophoresis used to monitor the enrichment culture of aerobic chemoorganotrophic bacteria from a hot spring cyanobacterial mat. Appl. Environ. Microbiol. **62:**3922–3928.
29. **Suzuki, M. T., and S. J. Giovannoni.** 1996. Bias caused by template annealing in the amplification of mixtures of 16S rRNA genes by PCR. Appl. Environ. Microbiol. **62:**625–630.
30. **Ward, D. M., M. M. Bateson, R. Weller, and A. L. Ruff-Roberts.** 1992. Ribosomal RNA analysis of microorganisms as they occur in nature. Adv. Microb. Ecol. **12:**219–286.
31. **Ward, D. M., M. J. Ferris, and M. M. Bateson.** Organization of native populations within hot spring microbial mat communities: need for a more ecological approach. *In* Proceedings of the 7th Symposium of the International Society for Microbial Ecology, Santos, Brazil, September 1995, in press.
32. **Ward, D. M., M. J. Ferris, S. C. Nold, M. M. Bateson, E. D. Kopczynski, and A. L. Ruff-Roberts.** 1994. Species diversity in hot spring microbial mats as revealed by both molecular and enrichment culture approaches—relationship between biodiversity and community structure, p. 33–44. *In* L. J. Stal and P. Caumette (ed.), Microbial mats: structure, development and environmental significance. Springer-Verlag KG, Berlin, Germany.
33. **Ward, D. M., R. Weller, and M. M. Bateson.** 1990. 16S rRNA sequences reveal uncultured inhabitants of a well-studied thermal community. FEMS Microbiol. Rev. **75:**105–116.
34. **Ward, D. M., R. Weller, and M. M. Bateson.** 1990. 16S rRNA sequences reveal numerous uncultured microorganisms in a natural community. Nature **345:**63–65.
35. **Weller, R., M. M. Bateson, B. K. Heimbuch, E. D. Kopczynski, and D. M. Ward.** 1992. Uncultivated cyanobacteria, *Chloroflexus*-like inhabitants, and spirochete-like inhabitants of a hot spring microbial mat. Appl. Environ. Microbiol. **58:**3964–3969.
36. **Weller, R., J. W. Weller, and D. M. Ward.** 1991. 16S rRNA sequences of uncultivated hot spring cyanobacterial mat inhabitants retrieved as randomly primed cDNA. Appl. Environ. Microbiol. **57:**1146–1151.